TISSUE ENGINEERING: Part C
Volume 18, Number 7, 2012

DOI: 10.1089/ten.tec.2011.0518

Tracking Hypoxic Signaling in Encapsulated Stem Cells

Suchit Sahai, B.S.,[1] Rachel McFarland,[2] Mathew L. Skiles, B.S.,[1] Denise Sullivan, B.S.,[1] Amanda Williams,[1] and James O. Blanchette, Ph.D.[1,3]

Oxygen is not only a nutrient but also an important signaling molecule whose concentration can influence the fate of stem cells. This study details the development of a marker of hypoxic signaling for use with encapsulated cells. Testing of the marker was performed with adipose-derived stem cells (ADSCs) in two-dimensional (2D) and 3D culture conditions in varied oxygen environments. The cells were genetically modified with our hypoxia marker, which produces a red fluorescent protein (DsRed-DR), under the control of a hypoxia-responsive element (HRE) trimer. For 3D culture, ADSCs were encapsulated in poly(ethylene glycol)–based hydrogels. The hypoxia marker (termed HRE DsRed-DR) is built on a recombinant adenovirus and ADSCs infected with the marker will display red fluorescence when hypoxic signaling is active. This marker was not designed to measure local oxygen concentration but rather to show how a cell perceives its local oxygen concentration. ADSCs cultured in both 2D and 3D were exposed to 20% or 1% oxygen environments for 96 h. In 2D at 20% O_2, the marker signal was not observed during the study period. In 1% O_2, the fluorescent signal was first observed at 24 h, with maximum prevalence observed at 96 h as 59% ± 3% cells expressed the marker. In 3D, the signal was observed in both 1% and 20% O_2. The onset of signal in 1% O_2 was observed at 4 h, reaching maximum prevalence at 96 h with 76% ± 4% cells expressing the marker. Interestingly, hypoxic signal was also observed in 20% O_2, with 13% ± 3% cells showing positive marker signal after 96 h. The transcription factor subunit hypoxia inducible factor-1α was tracked in these cells over the same time period by immunostaining and western blot analysis. Immunostaining results in 2D correlated well with our marker at 72 h and 96 h, but 3D results did not correlate well. The western blotting results in 2D and 3D correlated well with the fluorescent marker. The HRE DsRed-DR virus can be used to track the onset of this response for encapsulated, mesenchymal stem cells. Due to the importance of hypoxic signaling in determination of stem cell differentiation, this marker could be a useful tool for the tissue engineering community.

Introduction

Molecular oxygen serves as a metabolic substrate and signaling molecule for cells both *in vitro* and *in vivo*. Stems cells reside in a range of different microenvironments and the local oxygen concentration can help guide their differentiation. Ma *et al.* point out that mammalian embryogenesis and development take place at hypoxic conditions of 1.5%–8% O_2 and 2.3%–5.2% O_2, respectively.[1] In the literature, oxygen concentrations <5% have been described as hypoxic conditions.[1–3] Hypoxia can create a potentially lethal environment and limit cellular respiration and growth or, alternatively, enhance the production of specific extracellular matrix components and increase angiogenesis.[4] A hypoxic environment plays a substantial and critical role in many essential physiological and developmental pathways. It has been linked to maintenance, proliferation, survival, and differentiation of various types of stem cells and influences the lineage commitment of multipotent cells.[5–8]

Cell response to reduced oxygen tension is primarily regulated by hypoxia-inducible factors (HIFs).[9,10] HIFs are transcription factors that belong to the bHLH-PAS (basic Helix-Loop-Helix-PER-ARNT-SIM) family. HIF-1 is a heterodimer composed of HIF-1α and HIF-1β. HIF-1β, also referred to as aryl hydrocarbon receptor nuclear translocator (ARNT), is stable regardless of local oxygen tension whereas HIF-1α is only stable under hypoxic conditions. Under normoxia (high oxygen conditions), HIF-1α is rapidly degraded due to hydroxylation, which promotes ubiquitination and subsequent proteosomal degradation.[9–12] The amount of HIF-1α increases exponentially in cells as oxygen levels drop from 6% O_2.[12] HIF-1 regulates transcription of genes that contain hypoxia-responsive elements (HREs) in their promoters, introns, and/or 3′ enhancers. HIF-1 interacts with

[1]Biomedical Engineering Program, College of Engineering and Computing, University of South Carolina, Columbia, South Carolina.
[2]Department of Biomedical Engineering, Johns Hopkins University, Baltimore, Maryland.
[3]Department of Chemical Engineering, College of Engineering and Computing, University of South Carolina, Columbia, South Carolina.

HREs leading to transcription of oxygen-regulated genes like vascular endothelial growth factor (*VEGF*), *erythropoietin*, cytokine-inducible nitric oxide synthase (*iNOs*), and glycolytic enzymes that enhance cellular adaptation to hypoxia.[13–15] This oxygen-sensitive regulation of transcription allows cells to adapt to changing oxygen tensions or to survive in physiological environments where the oxygen level is always in the hypoxic range. It has been estimated that 5% or more of our genes are regulated by HIF-1. VEGF, basic fibroblast growth factor, angiopoietin 2, and platelet-derived growth factor are examples of angiogenic molecules whose expression is increased by HIF-1 activity.[16–20] Hypoxia and HIF-1 are also implicated in the recruitment of circulating angiogenic cells, critical in vascular remodeling.[21–24] Given the interest in driving vascularization of tissue engineering constructs, HIF-1 activity is an important event to monitor for cells in these scaffolds.

Most *in vitro* cell culture studies are conducted at atmospheric oxygen levels of ~20%, which far exceed the physiological levels. Since oxygen concentration is an important component of the stem cell "niche" that affects the behavior of stem cells, it is important to account for it while interpreting experiments.[25] The effect of oxygen on adipose-derived stem cells (ADSCs) has been explored in a number of recent studies.[26–28] ADSCs are multipotent, mesenchymal stem cells that can be isolated through lipoaspiration. ADSCs have been used to differentiate into chondrogenic, osteogenic, endothelial, cardiomyogenic, myogenic, adipogenic, and potentially neurogenic phenotypes with HIF-1 activity affecting many of these pathways.[26–33]

The design of a tissue engineering scaffold can also impact local oxygen levels for cells within the material. Hydrogels are an attractive choice as a scaffold material because their high water content facilitates transport of nutrients and waste products to and from the encapsulated cells. Poly(ethylene glycol) (PEG) hydrogels are broadly utilized in the field of tissue engineering and can be easily functionalized to create custom microenvironments for encapsulated cells.[34–42] Oxygen supply to cells in three-dimensional (3D) constructs is more complex than in 2D cultures as it is influenced by the chemistry of the scaffold material(s), scaffold dimensions, local oxygen tension, cell type, cell density, as well as by the mechanisms of transport, that is, diffusion or convection. Studies in 3D culture revealed that the oxygen concentration decreases from the periphery toward the center of the scaffolds, which correlates with cell density and cell viability.[43,44] The oxygen concentrations in the media and inside the scaffolds have been measured using oxygen-sensing dyes, oxygen microelectrodes, fluorescent probes, and microparticles.[45–50] Mathematical modeling approaches have been developed accounting for scaffold geometry and local oxygen tension to predict oxygen gradients inside the scaffolds.[51] These techniques to measure or predict oxygen concentration offer a great deal of information to the tissue engineering community. However, it is also important to know how cells react to their local oxygen concentration to predict changes in phenotype.

Because of the importance of how cells respond to the local oxygen and the role of HIF-1 in stem cell behavior, we developed a responsive, fluorescent hypoxia marker based on a recombinant adenovirus.[52] The sequence of a red fluorescent protein (DsRed-DR) was placed under the control of a minimal promoter and HRE trimer. This virus is referred to as HRE DsRed-DR. Expression of the fluorescent protein should match the expression of other HIF-1–regulated genes. HIF-1 regulates expression of antiapoptotic genes and secretion of numerous angiogenic factors. A system to track the onset of these events will assist tissue engineering efforts using a range of scaffold materials and culture in many different oxygen conditions. A number of techniques exist to measure the amount of HIF-1α in cells but many require that the cells be lysed or fixed. HIF-1 activity does not always correlate with the amount of HIF-1 protein or mRNA that compromises techniques measuring such quantities that seek to predict expression of HIF-regulated genes.

The objective of this study was to evaluate a responsive, fluorescent, hypoxia detection system and determine whether HIF activity can be tracked at a cellular level in both 2D and 3D cultures. ADSCs were selected due to their broad utilization in tissue engineering strategies and the influence of HIF signaling on ADSC phenotype. The experiments outlined in the following section were designed to examine the relationship between culture conditions and hypoxic signaling. A mechanism to continuously monitor HIF activity in encapsulated cells is a useful tool for the tissue engineering community.

Materials and Methods

Cell culture

Human ADSCs isolated from human lipoaspirate tissue were purchased from Invitrogen at passage 1. Cells were cultured in proprietary MesenPRO RS™ basal medium supplemented with MesenPRO RS Growth Supplement, 1% penicillin/streptomycin (Mediatech), and 2 mM L-glutamine (MP Biomedicals). Culture conditions for passaging were maintained at 95% air and 5% CO_2 at 37°C. For experiments, cells between passages 2 and 7 were used as recommended by the supplier.

Oxygen-controlled culture

Nitrogen-purged, programmable incubators were used to maintain constant oxygen levels for cellular studies (Napco Series 8000 WJ; Thermo Electron). Normoxic oxygen studies were maintained at 5% CO_2 and 20% oxygen and hypoxic studies were maintained at 5% CO_2 and 1% oxygen conditions. For 1% oxygen experiments, all media, buffered salt solutions, and fixatives to be used with cells were kept in vented tubes in the hypoxic incubator for 24 h prior to use so as to equilibrate the solutions to the appropriate dissolved oxygen concentration. Previous studies in our lab have shown this period to be sufficient to equilibrate the dissolved oxygen concentration.[52] All cell manipulation (media changes and imaging) was performed as quickly as possible to minimize exposure to atmospheric air. These procedures were kept under 10 min per day. Studies using a dissolved oxygen sensor tracked the change in dissolved oxygen levels in the media during this time and found that levels only increased from 0.3 mg/L (concentration equilibrated in 1% oxygen incubator) to 0.4 mg/L after 10 min outside of the incubator. The concentration had returned to 0.3 mg/L within 10 min of placement back in the incubator.

Infection of ADSCs and tracking hypoxic signaling

The preparation of the virus was briefly described earlier and is detailed in previously published studies.[52] As observed in those previous studies, the virus exhibited 100% infection efficiency with ADSCs. For marker studies, ADSCs were seeded into a 12-well tissue culture treated plate with the HRE DsRed-DR virus at a multiplicity of infection of 25. The plates were incubated overnight in static culture at 20% O_2 for the cells to attach to the surface and for the infection to take place. Both 2D and 3D samples were fluorescently imaged periodically over 96 h using a Nikon Eclipse Ti microscope (Nikon) and the Nikon NIS-Elements imaging software with consistent exposure times and fluorescent lamp intensities. Multiple images (three to four images for 2D samples and five to six images for 3D samples) from three independent studies were used to quantify the cells expressing positive marker signal.

Cell encapsulation for 3D experiments

PEG with an average molecular weight of 10,000 Da (Sigma-Aldrich) was functionalized by addition of methacrylate end groups resulting in PEG dimethacrylate (PEGDM). ADSCs were trypsinized, counted using a hemocytometer, and spun down in a microcentrifuge tube prior to removal of the media. Cells were then resuspended in a solution of 10 wt% PEGDM and 0.025 wt% 2-hydoxy-1-[4-(2-hydroxyethoxy)-phenyl]-2-methyl-1-propanone (Irgacure 2959; Ciba), which is a photoinitiator in Hank's balanced salt solution (HBSS; Mediatech, Inc). Each gel in these studies was designed to contain 400,000 dispersed ADSCs so enough cells were added to the PEGDM to create a concentration of 10,000 cells/μL. After resuspension of the cells, 40 μL of the PEGDM suspension was added to a 1 mL syringe and exposed to a 365 nm light source at an intensity of $7\ mW \cdot cm^{-2}$ for 10 min under sterile conditions. The resulting gels are cylindrical discs measuring 5 mm in diameter and 2 mm in height. The gels were transferred to a 24-well plate, washed in HBSS, and placed in 1.5 mL of media. The plates were cultured in the varied oxygen conditions on orbital shakers set to continuous rotation at 100 rpm. This encapsulation procedure has been shown previously to not have an adverse impact on viability for a range of cell types.[22–24]

Protein extraction and western blotting for HIF-1α

Total cell lysates were collected from the 2D and 3D samples with RIPA lysis buffer (Thermo Scientific) containing a protease and phosphatase inhibitor cocktail (Thermo Scientific), stirred on ice for 10 min, and sonicated for 15 min. The mixtures were then centrifuged at 14,000 rpm at 4°C for 15 min. The supernatants were collected and protein concentration was quantified using a Coomassie Plus Bradford Assay kit (Thermo Scientific) according to the manufacturers' instructions.

Western blotting was performed by sodium dodecyl sulfate-polyacrylamide gel electrophoresis with 50 μg of protein lysate loaded per lane of 4%–20% gradient gels followed by transfer to polyvinylidene fluoride membranes (Millipore). The membrane was first incubated in 5% dry milk and 1% bovine serum albumin (BSA) diluted in HBSS for 1 h at room temperature. The membrane was then washed twice for 10 min each in "wash 1" (0.1% Tween-20, 0.1% dry milk, and 0.1% BSA in HBSS). The membrane was then incubated with rabbit anti-HIF-1α antibody (1:1000; Santa Cruz Biotechnology) and rabbit anti-β-actin antibody (1:1000; Santa Cruz Biotechnology) for 2 h at room temperature. The membrane was then washed three times for 10 min each in "wash 1." Membranes were then incubated with peroxidase-conjugated, goat, anti-rabbit IgG (1:5000; Rockland Immunochemicals) for 2 h at room temperature. Membranes were then washed three times for 10 min each in "wash 2" (0.1% Tween-20 in HBSS). Protein detection was achieved by 5-min incubation in a chemiluminescence reagent, Super-Signal West Pico Substrate (Thermo Scientific). Bands were then detected using ChemiDoc™ XRS^+ System with Image Lab™ image acquisition and analysis software (Bio-Rad). With densitometry analysis, the expression of proteins was normalized to β-actin to account for percent of intensity optical density (%IOD) fold difference of HIF-1α protein expression. All incubation steps and washes were performed on an orbital shaker set to continuous rotation at 100 rpm. The statistics shown represent results obtained from three independent studies.

Immunostaining for HIF-1 activity

About 100,000 ADSCs were plated in flat-bottom 96-well plates for 2D experiments. The previously described, ADSC-containing PEG gels were used for 3D experiments. The samples were maintained in 1% and 20% O_2 for a period of 96 h. To prepare the cells for staining, samples were fixed after 24, 48, 72, and 96 h with 4% paraformaldehyde (Thermo Fisher) on ice for 30 min and washed twice with HBSS. Staining was performed every 24 h during the 4-day period. Cells were permeabilized with 0.1% Triton X (EMD Chemicals) for 30 min and then washed successively in 5% BSA (EMD Chemicals) and 5% normal donkey serum (EMD Chemicals) for 1 h each. An overnight incubation at 4°C with polyclonal rabbit antibody to HIF-1α (1:1000; Santa Cruz Biotechnology) was followed by two, 15-min washes in 1% BSA and a 1-h incubation in 5% normal donkey serum. A fluorescently labeled, goat, anti-rabbit secondary antibody (1:1000; Rockland Immunochemicals) was added for an hour followed by final washes in 1% BSA in HBSS. Samples were fluorescently imaged with the instrumentation and software previously mentioned. Multiple images (three to four images for 2D samples and five to six images for 3D samples) from three independent samples were analyzed to quantify the number of cells expressing HIF-1α.

Viability of ADSCs

Live/Dead® staining kit (Invitrogen) was used to test the viability of the samples. Fluorescent dyes indicate esterase activity (observed as green signal in live cells) or loss of nuclear membrane integrity (observed as red signal in dead cells). The 2D and 3D samples were in culture conditions similar to the previous experiments and the staining was performed in accordance with the manufacturer's guidelines. Results are given as a percentage of viable cells based on analysis of three independent studies.

Statistical analysis

Statistical analysis was performed using Graphpad Prism 4.01 (GraphPad Software, Inc.). Experimental results were expressed as the mean ± standard deviation. All the collected data were analyzed by two-way analysis of variance for comparisons and p-values < 0.05 were defined as statistically significant differences.

Results

HIF-1α immunostaining

The HIF-1α staining (green) was primarily focused in the cytoplasm of ADSCs. In 2D at 20% O_2, no staining was evident during the entire time course. A representative image after 96 h of culture is shown in Figure 1A. In 1% O_2, no signal was observed at 24 and 48 h. About 56% ± 3% and 61% ± 4% cells stained positive for HIF-1α at 72 and 96 h, respectively. Representative images are shown in Figure 1B and C. In 3D, no signal was observed at 24 and 48 h at both 1% and 20% O_2. In 1% O_2, staining was observed at 72 and 96 h with 13% ± 2% and 25% ± 4% cells staining positive, respectively. The representative image at 96 h in 1% O_2 is shown in Figure 1D1 and D2 (overlay image). Immunostaining was also observed at 20% O_2 in 3D, with 9% ± 2% and 11% ± 3% cells stained positive for HIF-1α at 72 and 96 h, respectively, as in shown in Figure 1E1 and E2 (overlay image). These results are summarized in Figure 1F.

Hypoxia marker signaling

In 2D at 20% O_2, there was no marker signal throughout the study period of 4 days. At 1% O_2, the onset of the signal was seen at 8 h with 4% ± 1% cells showing positive red fluorescence signal for HIF-1α activation. Signal progression increased with 11% ± 3%, 17% ± 4%, 26% ± 3%, 54% ± 2%, and 59% ± 3% of cells showing positive marker signal at 12, 24, 48, 72, and 96 h, respectively. A representative image for each time point is shown in Figure 2 (A1–A6). In 3D at 1% O_2, we observed the onset of the marker signal at 4 h with 5% ± 1% cells expressing positive signal. The prevalence of the signal increased over time with 9% ± 3%, 15% ± 5%, 32% ± 4%, 54% ± 2%, 62% ± 4%, and 76% ± 3% cells expressing positive marker signal at 8, 12, 24, 48, 72, and 96 h, respectively. Representative images for each time point are shown in Figure 2 (B1–B7). Marker signal was also observed in 3D at 20% O_2. The onset of the signal was at 24 h with 4% ± 2% cells showing positive marker signal. The prevalence of the signal increased over time with 7% ± 2%, 9% ± 4%, and 13% ± 3% cells expressing positive marker signal at 48, 72, and 96 h,

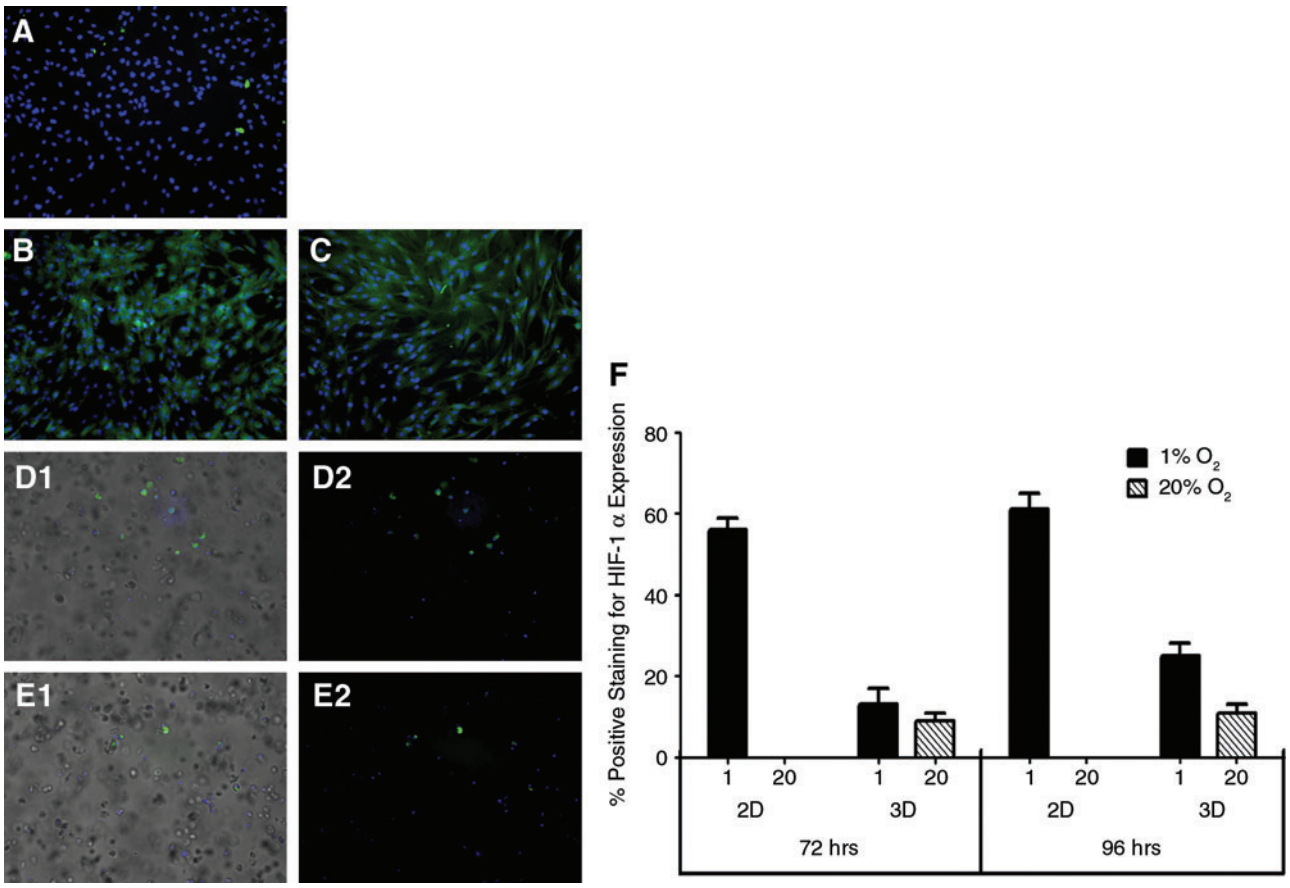

FIG. 1. Immunostaining for HIF-1α: HIF-1α, if present, was stained green. As a counterstain, cell nuclei labeled with DAPI appear blue. **(A)** At 20% O_2, there was no significant staining at 96 h in 2D. **(B, C)** shows cells in 2D at 1% O_2 stained for HIF-1α at 72 and 96 h, respectively. **(D, E)** HIF-1α staining in 3D. **(D1)** Immunostaining in 1% at 96 h (**D2** is an overlay image). **(E1)** is the representative image of staining at 20% O_2 at 96 h (**E2** is an overlay image). Quantification of HIF-1α–expressing cells **(F)** from each of the studies **(A–E)**. HIF, hypoxia-inducible factor; DAPI, 4′,6′-diamidino-2-phenylindole; 2D, two-dimensional. Color images available online at www.liebertonline.com/tec

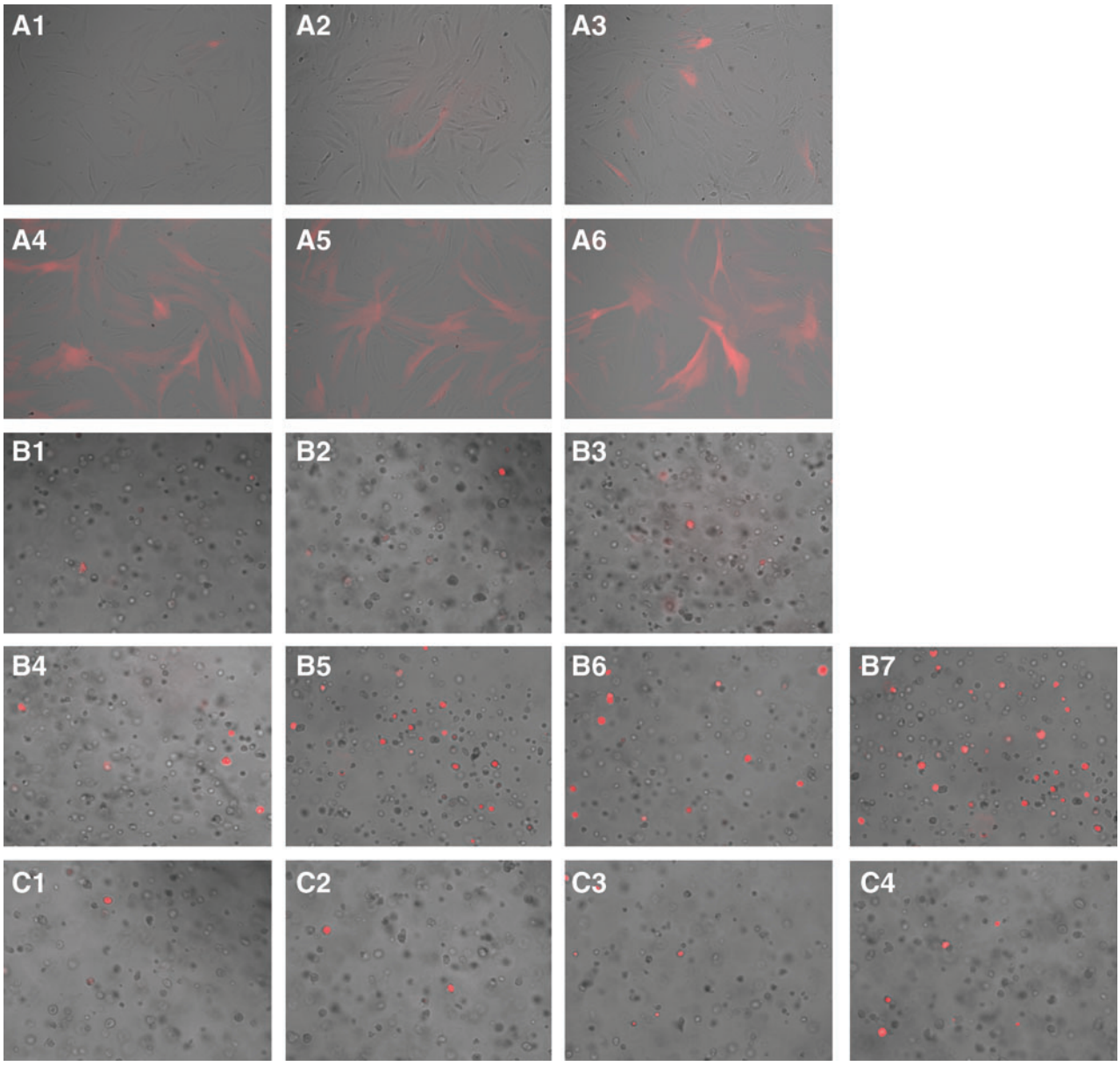

FIG. 2. Hypoxia marker progression. **(A1–A6)** shows marker progression in 2D at 1% O_2 through 8, 12, 24, 48, 72, and 96 h, respectively. In 3D, onset of marker signal was first observed at 4 h **(B1)** and the prevalence of the signal increased over time, as shown in **(B2–B7)** corresponding to 8, 12, 24, 48, 72, and 96 h of culture, respectively. In 3D, signal was also observed in 20% O_2. These images **(C1–C4)** show marker progression at 24, 48, 72, and 96 h, respectively. Color images available online at www.liebertonline.com/tec

respectively (Fig. 2C1–C4). The above results are summarized in Figure 3.

Quantification of HIF-1α protein

Western blotting was performed to quantify the amount of HIF-1α protein expressed in 2D and 3D culture conditions under 1% and 20% O_2. Figure 4A shows bands for HIF-1α protein in 1% O_2 in both 2D and 3D culture conditions. Quantification of these results using %IOD measurements and normalizing HIF-1α expression with β-actin expression showed an increase in HIF-1α expression over time. In 3D at 1% O_2, we saw a %IOD fold difference of 6.01 ± 0.42, 10.31 ± 0.34, 11.31 ± 0.453, and 11.39 ± 0.31 at 24, 48, 72, and 96 h, respectively. In 2D at 1% O_2, we observed a %IOD fold difference of 1.31 ± 0.21, 2.52 ± 0.34, 6.78 ± 0.23, and 7.11 ± 0.36 at 24, 48, 72, and 96 h, respectively. Figure 4B shows protein levels of HIF-1α examined at 20% O_2 in both 2D and 3D. In 2D, we observed no expression of HIF-1α throughout the study period. In 3D the expression pattern was 0.61 ± 0.246, 3.32 ± 0.283, 3.98 ± 0.183, and 4.01 ± 0.15 %IOD fold difference at 24, 48, 72, and 96 h, respectively. The above results are summarized in Figure 4C.

ADSC viability

Viability of ADSCs in 2D and 3D cultures at both 1% and 20% O_2 was observed every 24 h for the time period of 4 days. In 2D at 20% O_2, the % viability was $99\% \pm 0.2\%$, $98\% \pm 0.6\%$, $98\% \pm 0.4\%$, and $98\% \pm 0.3\%$, at 24, 48, 72, and

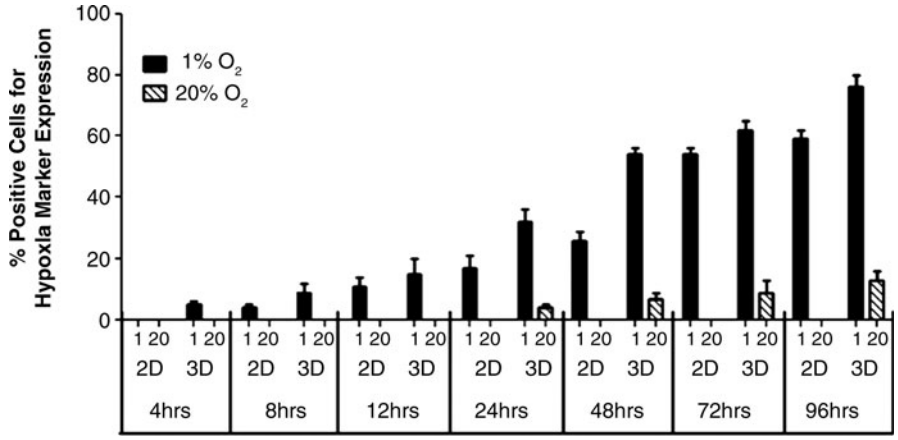

FIG. 3. Quantification of cells positive for marker signal. The graph quantifies the percent positive cells expressing hypoxia marker signal in 2D and 3D conditions in both 1% and 20% O_2 conditions.

96 h, respectively. At 1% O_2 incubation, the % viability was observed at 99% ± 0.4%, 99% ± 0.02%, 98% ± 0.5%, and 98% ± 0.3% at 24, 48, 72, and 96 h, respectively. For 3D cultures in 20% O_2, 99% ± 0.4%, 99% ± 0.3%, 98% ± 0.6%, and 97% ± 0.4% viability was observed at 24, 48, 72, and 96 h, respectively. Finally, for 3D cultures in 1% O_2, 99% ± 0.2%, 98% ± 0.4%, 97% ± 0.3%, and 97% ± 0.4% cell viability were observed at 24, 48, 72, and 96 h, respectively.

Discussion

Immunostaining results in 2D at 20% O_2 did not show any staining for HIF-1α at any of the time points, which correlates with our marker. At 1% O_2, signal was only observed at 72 and 96 h, which also correlated well with our marker. Interestingly in 3D, we observed immunostaining and hypoxia marker signal (Fig. 2C1–C4) in both 1% and 20% O_2. The results in 20% oxygen show the impact of the PEG material on oxygen diffusion. The immunostaining in 3D did not correlate as well with our marker, as a lower percentage of cells stained positive for HIF-1α (Figs. 1F and 3) than displayed the fluorescent marker signal under the same conditions.

The discrepancy could be due to limited diffusion of the primary and secondary antibodies through the scaffold. Crosslinked PEG hydrogels formed from macromers of molecular weight 10 kDa exhibit a mesh size of 7.78 nm.[53] The hydrodynamic radius of our antibodies should be below this size but the pore size is heterogeneous and diffusion may have been impeded. Limitations in protein diffusion were not observed in our western blotting experiments. The protein quantity yield of 400,000 cells lysed in 2D culture was equivalent to that obtained when lysates were collected from gels containing 400,000 cells following 3D culture. Quantification of HIF-1α by western blot displayed higher intensity bands in 3D than 2D at 1% O_2 at each of the time points (Fig. 4A). At 20% O_2, there were no bands for HIF-1α in 2D at any time points. Some HIF-1α was detected in 3D cultures (Fig. 4B). Figure 4C shows the %IOD fold difference in HIF-1α protein expression. Detection of HIF-1α by immunocytochemistry should not produce significantly different results from detection by western blotting and the two matched up quite well for 2D studies. The lack of correlation within the scaffold highlights the utility of the HRE DsRed-DR marker as it did not exhibit the same issues and matched the trend seen with the western blot results.

The cellular response to HIF-1 is not homogeneous across cell types, with degree of stabilization and upregulated target genes varying between and within tissues.[54,55] In this respect, the amount of HIF-1α does not necessarily correlate with HIF-1 activity. If this was occurring with our ADSCs, then a difference would be expected between the signal from

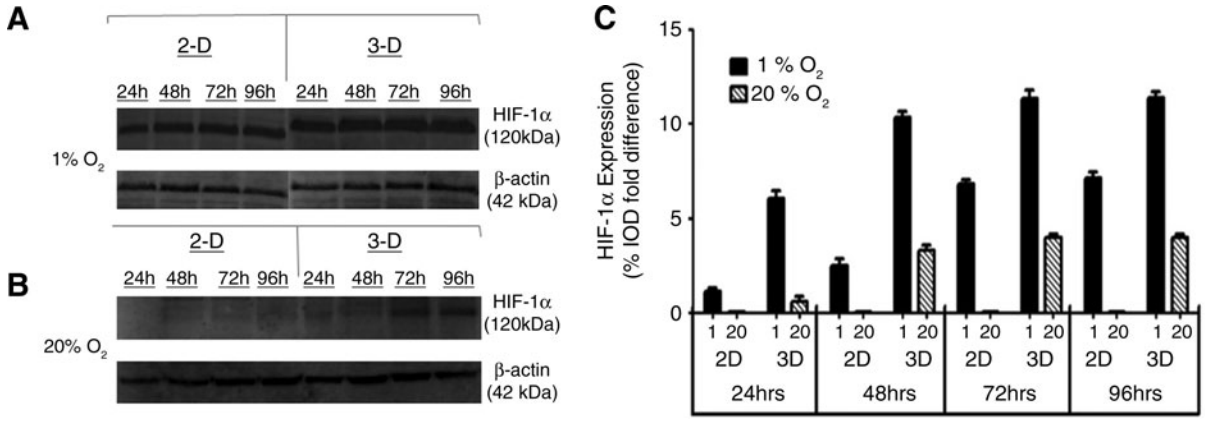

FIG. 4. Western blot for HIF-1α and β-actin. Results are shown for ADSCs cultured in 1% O_2 **(A)** and 20% O_2 **(B)**. These results are quantified in **(C)**. ADSCs, adipose-derived stem cells; IOD, intensity optical density.

the marker and both methods used to detect HIF-1α quantity instead of just 3D immunocytochemical results.

Extended exposure to hypoxia can affect the viability of cells. Our results showed that more than 95% of cells were viable at 1% O_2 in both 2D and 3D through 4 days of culture, suggesting that the low oxygen environment triggered HIF-1 activity but not a large drop in viability. This could be explained by the low metabolic activity of ADSCs and that stabilization of HIF-1α protects cells against necrosis helping them to survive under acute or chronic hypoxia.[56]

As stated in the introduction, our goal was to establish whether the HRE DsRed-DR marker virus could be used to track HIF-1 activity in encapsulated ADSCs and whether expression of the red fluorescent protein correlated with HIF-1α detected by traditional methods. The marker measures HIF activity rather than the amount of HIF-1α protein as measured with western blotting and immunocytochemical detection. A lag was expected between the stabilization of the transcription factor and expression of the fluorescent protein but it proved to be brief as the fluorescent signal was observed as early as 4 h after exposure to hypoxic conditions. Our results show that detection of the signal is certainly possible and that image capture conditions can be established that allow the observed signal to correlate with HIF-1α levels. These image capture conditions did not lead to background signal in cells when no HIF-1α was detected by other methods. We can monitor HIF activity in the same population of cells over time and this can be done in a 3D culture environment without disruption of the scaffold.

The majority of cell culture studies have been performed on 2D surfaces such as tissue culture plates/flasks because of the ease, convenience, and high cell viability of 2D culture. These traditional 2D cultures cannot be used to faithfully mimic the microenvironment of the particular tissue of interest. The combination of 3D scaffolds and living cells is used to fill defect sites and support the transplanted cells. The material(s) selected for the scaffold and how it is synthesized influence the diffusion of oxygen and nutrients to the cells and this is a major limitation in tissue engineering.[43] Gradients of oxygen concentration can form within materials and this will affect cellular differentiation or cell fate decisions.[57–59] This marker system was developed to identify hypoxic signaling within these environments and to track this response at a cellular level without the need to disrupt the integrity of the scaffold or cells.

It is clear from previous studies that oxygen concentration and the cell response to the local oxygen tension are important parameters to track when devising novel, stem cell–based therapeutic systems. Our marker does not measure the oxygen concentration, but more importantly helps in the identification of a cellular response at low oxygen conditions. Several techniques have been applied to measure the spatial distribution of oxygen within tissues using blood-gas analyzers, dissolved oxygen probes, and fluorescent/luminescent particles.[48–50,60,61] These systems offer high levels of sensitivity and specificity, but do not show how the cells respond to their local oxygen environment. The marker system described here can complement such techniques and offers great potential as a tool to track biological responses in tissue engineering studies.

Studies have shown that there may be a strong dependence of cellular metabolic activity and oxygen consumption rate on the scaffolding material and geometry, presumably due to altered cell–material interactions in the scaffold.[46,62] Therefore in the future, it would be interesting to evaluate the effect on the prevalence and onset of the marker signal within different scaffold materials for a range of cell densities. Due to the link between local oxygen levels and cell behavior, these gradients can cause heterogeneous differentiation of cells within tissue engineering scaffolds if steps are not taken to address the creation of these gradients. Future studies will take advantage of the versatility of our responsive hypoxia marker to show dynamic correlations between cell fate and function with oxygen concentration in engineered tissues in 2D as well as 3D environments.

Disclosure Statement

No competing financial interests exist.

References

1. Ma, T., Grayson, W.L., Frohlich, M., and Vunjak-Novakovic, G. Hypoxia and stem cell-based engineering of mesenchymal tissue. Biotechnol Prog **25,** 32, 2009.
2. Fehrer, C., Brunauer, R., Laschober, G., Unterluggauer, H., Reitinger, S., Kloss, F., Gully, C., Gabner, R., and Lepperdinger, G. Reduced oxygen tension attenuates differentiation capacity of human mesenchymal stem cells and prolongs their lifespan. Aging Cell **6,** 745, 2007.
3. Ren, H., Cao, Y., Zhao, Q., Li, J., Zhou, C., Liao, L., Jia, M., Zhao, Z., Cai, H., Han, Z.C., Yang, R., Chen, G., and Zhao, R.C. Proliferation and differentiation of bone marrow stromal cells under hypoxic conditions. Biochem Biophys Res Commun **347,** 12, 2006.
4. Semenza, G.L. Expression of hypoxia-inducible factor 1: mechanisms and consequences. Biochem Pharmacol **59,** 47, 2000.
5. Ivanovic, Z. Hypoxia or *in situ* normoxia: the stem cell paradigm. J Cell Physiol **219,** 271, 2009.
6. Abdollahi, H., Harris, L.J., Zhang, P., McIlhenny, S., Srinivas, V., Tulenko, T., and DiMuzio, P.J. The role of hypoxia in stem cell differentiation and therapeutics. J Surg Res **165,** 112, 2011.
7. Lin, Q., Kim, Y., Alarcon, R.M., and Yun, Z. Oxygen and cell fate decisions. Gene Regul Syst Bio **2,** 43, 2008.
8. Malda, J., Klein, T.J., and Upton, Z. The roles of hypoxia in the *in vitro* engineering of tissues. Tissue Eng **13,** 2153, 2007.
9. Semenza, G. Signal transduction to hypoxia-inducible factor 1. Biochem Pharmacol **64,** 993, 2002.
10. Semenza, G.L. Oxygen homeostasis. Syst Biol Med **2,** 336, 2010.
11. Semenza, G.L. Hypoxia-inducible factor 1: master regulator of O_2 homeostasis. Curr Opin Genet Dev **8,** 588, 1998.
12. Jiang, B.-H., Rue, E., Wang, G.L., Roe, R., and Semenza, G.L. Dimerization, DNA binding, and transactivation properties of hypoxia-inducible factor 1. J Biol Chem **271,** 17771, 1996.
13. Sharp, F.R., and Bernaudin, M. HIF-1 and oxygen sensing in the brain. Nat Rev Neurosci **5,** 437, 2004.
14. Hwang, J.M., Weng, Y.J., Lin, J.A., Bau, D.T., Ko, F.Y., Tsai, F.J., Tsai, C.H., Wu, C.H., Lin, P.C., Huang, C.Y., and Kuo, W.W. Hypoxia-induced compensatory effect as related to Shh and HIF-1alpha in ischemia embryo rat heart. Mol Cell Biochem **311,** 179, 2008.
15. Wang, Y., Wan, C., Deng, L., Liu, X., Cao, X., Gilbert, S.R., Bouxsein, M.L., Faugere, M.C., Guldberg, R.E., Gerstenfeld, L.C., Haase, V.H., Johnson, R.S., Schipani, E., and Clemens,

T.L. The hypoxia inducible factor alpha pathway couples angiogenesis to osteogenesis during skeletal development. J Clin Invest **117,** 1616, 2007.
16. Forsythe, J.A., Jiang, B.H., Iyer, N.V., Agani, F., Leung, S.W., Koos, R.D., and Semenza, G.L. Activation of vascular endothelial growth factor gene transcription by hypoxia-inducible factor 1. Mol Cell Biol **16,** 4604, 1996.
17. Kelly, B.D., Hackett, S.F., Hirota, K., Oshima, Y., Cai, Z., Berg-Dixon, S., Rowan, A., Yan, Z., Campochiaro, P.A., and Semenza, G.L. Cell type-specific regulation of angiogenic growth factor gene expression and induction of angiogenesis in nonischemic tissue by a constitutively active form of hypoxia-inducible factor 1. Circ Res **93,** 1074, 2003.
18. Ceradin, D.J., Kulkarni, A.R., Callaghan, M.J., Tepper, O.M., Bastidas, N., Kleinman, M.E., Capla, J.M., Galiano, R.D., Levine, J.P., and Gurtner, G.C. Progenitor cell trafficking is regulated by hypoxic gradients through HIF-1 induction of SDF-1. Nat Med **10,** 858, 2004.
19. Manalo, D.J., Rowan, A., Lavoie, T., Natarajan, L., Kelly, B.D., Ye, S.Q., Garcia, J.G., and Semenza, G.L. Transcriptional regulation of vascular endothelial cell responses to hypoxia by HIF-1. Blood **105,** 659, 2005.
20. Simon, M.P., Tournaire, R., and Pouyssegur, J. The angiopoietin-2 gene of endothelial cells is up-regulated in hypoxia by a HIF binding site located in its first intron and by the central factors GATA-2 and Ets-1. J Cell Physiol **217,** 809, 2008.
21. Asahara, T., Takahashi, T., Masuda, H., Kalka, C., Chen, D., Iwaguro, H., Inai, Y., Silver, M., and Isner, J.M. VEGF contributes to postnatal neovascularization by mobilizing bone marrow-derived endothelial progenitor cells. EMBO J **18,** 3964, 1999.
22. Grant, M.B., May, W.S., Caballero, S., Brown, G.A., Guthrie, S.M., Mames, R.N., Byrne, B.J., Vaught, T., Spoerri, P.E., Peck, A.B., and Scott, E.W. Adult hematopoietic stem cells provide functional hemangioblast activity during retinal neovascularization. Nat Med **8,** 607, 2002.
23. Kinnaird, T., Stabile, E., Burnett, M.S., Lee, C.W., Barr, S., Fuchs, S., and Epstein, S.E. Marrow-derived stromal cells express genes encoding a broad spectrum of arteriogenic cytokines and promote *in vitro* and *in vivo* arteriogenesis through paracrine mechanisms. Circ Res **94,** 678, 2004.
24. Kinnaird, T., Stabile, E., Burnett, M.S., Lee, C.W., Barr, S., Fuchs, S., and Epstein, S.E. Local delivery of marrow-derived stromal cells augments collateral perfusion through paracrine mechanisms. Circulation **109,** 1543, 2004.
25. Moore, K.A., and Lemischka, I.R. Stem cells and their niches. Science **311,** 1880, 2006.
26. Bhang, S.H., Cho, S.W., La, W.G., Lee, T.J., Yang, H.S., Sun, A.Y., Baek, S.H., Rhie, J.W., and Kim, B.S. Angiogenesis in ischemic tissue produced by spheroid grafting of human adipose-derived stromal cells. Biomaterials **32,** 2734, 2011.
27. Lee, J.H., and Kemp, D.M. Human adipose-derived stem cells display myogenic potential and perturbed function in hypoxic conditions. Biochem Biophys Res Commun **341,** 882, 2006.
28. Wang, D.W., Fermor, B., Gimble, J.M., Awad, H.A., and Guilak, F. Influence of oxygen on the proliferation and metabolism of adipose derived adult stem cells. J Cell Physiol **204,** 184, 2005.
29. Liu, G., Cheng, Y., Guo, S., Feng, Y., Li, Q., Jia, H., Wang, Y., Tong, L., and Tong, X. Transplantation of adipose-derived stem cells for peripheral nerve repair. Int J Mol Med **28,** 565, 2011.
30. Zuk, P.A., Zhu, M., Mizuno, H., Huang, J., Futrell, J.W., Katz, A.J., Benhaim, P., Lorenz, H.P., and Hedrick, M.H. Multilineage cells from human adipose tissue: implications for cell based therapies. Tissue Eng **7,** 211, 2001.
31. Fraser, J.K., Wulur, I., Alfonso, Z., and Hedrick, M.H. Fat tissue: an underappreciated source of stem cells for biotechnology. Trends Biotechnol **24,** 150, 2006.
32. Schaffler, A., and Buchler, C. Concise review: adipose tissue-derived stromal cells-basic and clinical implications for novel cell-based therapies. Stem Cells **25,** 818, 2007.
33. Bunnell, B.A., Flaat, M., Gagliardi, C., Patel, B., and Ripoll, C. Adipose-derived stem cells: isolation, expansion and differentiation. Methods **45,** 115, 2008.
34. Buxton, A.N., Zhu, J., Marchant, R., West, J.L., Yoo, J.U., and Johnstone, B. Design and characterization of poly(ethylene glycol) photopolymerizable semi-interpenetrating networks for chondrogenesis of human mesenchymal stem cells. Tissue Eng **13,** 2549, 2007.
35. Lin-Gibson, S., Bencherif, S., Cooper, J.A., Wetzel, S.J., Antonucci, J.M., Vogel, B.M., Horkay, F., and Washburn, N.R. Synthesis and characterization of PEG dimethacrylates and their hydrogels. Biomacromolecules **5,** 1280, 2004.
36. Weber, L.M., and Anseth, K.S. Hydrogel encapsulation environments functionalized with extracellular matrix interactions increase islet insulin secretion. Matrix Biol **27,** 667, 2008.
37. Salinas, C.N., Cole, B.B., Kasko, A.M., and Anseth, K.S. Chondrogenic differentiation potential of human mesenchymal stem cells photoencapsulated within poly(ethylene glycol)-arginine-glycine-aspartic acid-serine thiol-methacrylate mixed-mode networks. Tissue Eng **13,** 1025, 2007.
38. Benoit, D.S., Durney, A.R., and Anseth, K.S. The effect of heparin-functionalized PEG hydrogels on three-dimensional human mesenchymal stem cell osteogenic differentiation. Biomaterials **28,** 66, 2007.
39. Hwang, N.S., Kim, M.S., Sampattavanich, S., Baek, J.H., Zhang, Z., and Elisseeff, J. Effects of three-dimensional culture and growth factors on the chondrogenic differentiation of murine embryonic stem cells. Stem Cells **24,** 284, 2006.
40. Ford, M.C., Bertram, J.P., Hynes, S.R., Michaud, M., Li, Q., Young, M., Segal, S.S., Madri, J.A., and Lavik, E.B. A macroporous hydrogel for the coculture of neural progenitor and endothelial cells to form functional vascular networks *in vivo*. Proc Natl Acad Sci U S A **103,** 2512, 2006.
41. Nuttelman, C.R., Tripodi, M.C., and Anseth, K.S. *In vitro* osteogenic differentiation of human mesenchymal stem cells photoencapsulated in PEG hydrogels. J Biomed Mater Res A **68,** 773, 2004.
42. Stosich, M.S., Bastian, B., Marion, N.W., Clark, P.A., Reilly, G., and Mao, J.J. Vascularized adipose tissue grafts from human mesenchymal stem cells with bioactive cues and microchannel conduits. Tissue Eng **13,** 2881, 2007.
43. Volkmer, E., Drosse, I., Otto, S., Stangelmayer, A., Stengele, M., Kallukalam, B.C., Mutschler, W., and Schieker, M. Hypoxia in static and dynamic 3-D culture systems for tissue engineering of bone. Tissue Eng Part A **14,** 1331, 2008.
44. Radisic, M., Malda, J., Epping, E., Geng, W., Langer, R., and Vunjak-Novakovic, G. Oxygen gradients correlate with cell density and cell viability in engineered cardiac tissue. Biotechnol Bioeng **93,** 332, 2006.
45. Kellner, K., Liebsch, G., Klimant, I., Wolfbeis, O.S., Blunk, T., Schulz, M.B., and Gopferich, A. Determination of oxygen gradients in engineered tissue using a fluorescent sensor. Biotechnol Bioeng **80,** 73, 2002.

46. Malda, J., Rouwkema, J., Martens, D.E., Le, E.P., Kooy, F.K., Tramper, J., van Blitterswijk, C.A., and Riesle, J. Oxygen gradients in tissue-engineered PEGT/PBT cartilaginous constructs: measurement and modeling. Biotechnol Bioeng **86,** 9, 2004.
47. Cochran, D.M., Fukumura, D., Ancukiewicz, M., Carmeliet, P., and Jain, R.K. Evolution of oxygen and glucose concentration profiles in a tissue-mimetic culture system of embryonic stem cells. Ann Biomed Eng **34,** 1247, 2006.
48. Revsbech, N.P., and Ward, D.M. Oxygen microelectrode that is insensitive to medium chemical composition: use in an acid microbial mat dominated by cyanidium caldarium. Appl Environ Microbiol **45,** 755, 1983.
49. Krihak, M.K., and Shahriari, M.R. Highly sensitive, all solid state fibre optic oxygen sensor based on the sol-gel coating technique. Electron Lett **32,** 240, 1996.
50. Acosta, M.A., Leki, P.Y., Kostov, Y.V., and Leach, J. B. Fluorescent microparticles for sensing cell microenvironment oxygen levels within 3D scaffolds. Biomaterials **30,** 3068, 2009.
51. Sengers, B.G., Taylor, M., Please, C.P., and Oreffo, R.O.C. Computational modeling of cell spreading and tissue regeneration in porous scaffolds. Biomaterials **13,** 1926, 2007.
52. Skiles, M.L., Fancy, R., Topiwala, P.S., Sahai, S., and Blanchette, J.O. Correlating hypoxia with insulin secretion using a fluorescent hypoxia detection system. J Biomed Mater Res B Appl Biomater **97,** 148, 2011.
53. Lin, S., Sangaj, N., Razafiarison, T., Zhang, C., and Varghese, S. Influence of physical properties of biomaterials on cellular behavior. Pharm Res **28,** 1422, 2011.
54. Bracken, C.P., Fedele, A.O., Linke, S., Balrak, W., Lisy, K., Whitelaw, M.L., and Peet, D.J. Cell-specific regulation of hypoxia-inducible factor (HIF)-1alpha and HIF-2alpha stabilization and transactivation in a graded oxygen environment. J Biol Chem **281,** 22575, 2006.
55. Lendahl, U., Lee, K.L., Yang, H., and Poellinger, L. Generating specificity and diversity in the transcriptional response to hypoxia. Nat Rev Genet **10,** 821, 2009.
56. Ginouves, A., Ilc, K., Macias, N., Pouyssegur, J., and Berra, E. PHDs overactivation during chronic hypoxia "desensitizes" HIF alpha and protects cells from necrosis. Proc Natl Acad Sci U S A **105,** 4745, 2008.
57. Malladi, P., Xu, Y., Chiou, M., Giaccia, A.J., and Longaker, M.T. Effect of reduced oxygen tension on chondrogenesis and osteogenesis in adipose-derived mesenchymal cells. Am J Physiol Cell Physiol **290,** C1139, 2006.
58. Mohyeldin, A., Garzon-Muvdi, T., and Hinojosa, A.Q. Oxygen in stem cell biology: a critical component of the stem cell niche. Cell Stem Cell **7,** 150, 2010.
59. Grayson, W.L., Zhao, F., Bunnell, B., and Ma, T. Hypoxia enhances proliferation and tissue formation of human mesenchymal stem cells. Biochem Biophys Res Commun **358,** 948, 2007.
60. Zhao, F., Pathi, P., Grayson, W., Xing, Q., Locke, B.R., and Ma, T. Effects of oxygen transport on 3-D human mesenchymal stem cell metabolic activity in perfusion and static cultures: experiments and mathematical model. Biotechnol Prog **21,** 1269, 2005.
61. Butt, O.I., Carruth, R., Kutala, V.K., Kuppusamy, P., and Moldovan, N.I. Stimulation of peri-implant vascularization with bone marrow-derived progenitor cells: monitoring by *in vivo* EPR oximetry. Tissue Eng **13,** 2053, 2007.
62. Cukierman, E., Pankov, R., and Yamada, K.M. Cell interactions with three-dimensional matrices. Curr Opin Cell Biol **14,** 633, 2002.

Address correspondence to:
James O. Blanchette, Ph.D.
Biomedical Engineering Program
College of Engineering and Computing
University of South Carolina
2C02 Swearingen, 301 Main St.
Columbia, SC 29208

E-mail: blanchej@cec.sc.edu

Received: September 12, 2011
Accepted: January 17, 2012
Online Publication Date: February 28, 2012